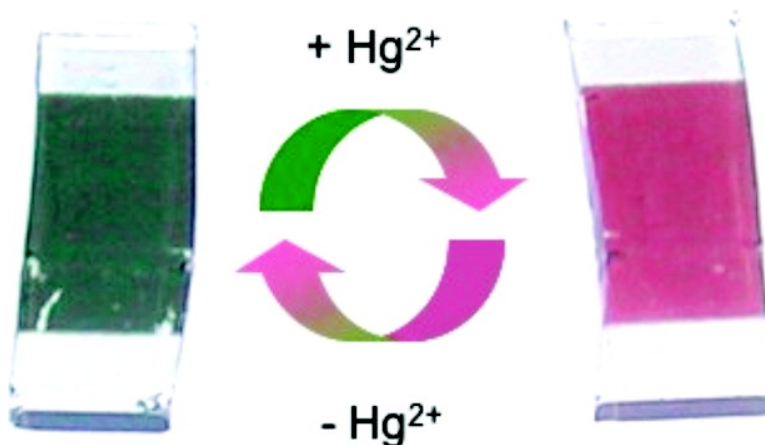


Reversible Colorimetric Probes for Mercury Sensing

Eugenio Coronado, Jos R. Galn-Mascars, Carlos Mart-Gastaldo, Emilio Palomares, James R. Durrant, Ramn Vilar, M. Gratzel, and Md. K. Nazeeruddin

J. Am. Chem. Soc., **2005**, 127 (35), 12351-12356 • DOI: 10.1021/ja0517724 • Publication Date (Web): 11 August 2005

Downloaded from <http://pubs.acs.org> on March 25, 2009



More About This Article

Additional resources and features associated with this article are available within the HTML version:

- Supporting Information
- Links to the 39 articles that cite this article, as of the time of this article download
- Access to high resolution figures
- Links to articles and content related to this article
- Copyright permission to reproduce figures and/or text from this article

[View the Full Text HTML](#)

Reversible Colorimetric Probes for Mercury Sensing

Eugenio Coronado,[†] José R. Galán-Mascarós,[†] Carlos Martí-Gastaldo,[†]
Emilio Palomares,^{*†‡} James R. Durrant,[‡] Ramón Vilar,[§] M. Gratzel,^{||} and
Md. K. Nazeeruddin^{||}

Contribution from the Institut de Ciència Molecular (IcMol), Universitat de València, 46100-Burjassot, Valencia, Spain, Centre for Electronic Materials and Devices, Department of Chemistry, Imperial College London, Exhibition Road, London SW7 2AY, U.K., ICREA and Institute of Chemical Research of Catalonia (ICIQ), 43007 Tarragona, Spain, and Laboratory for Photonics and Interfaces, Institute of Molecular and Biological Chemistry, School of Basic Sciences, Swiss Federal Institute of Technology, CH-1015 Lausanne, Switzerland

Received March 21, 2005; E-mail: .es

Abstract: The selectivity and sensitivity of two colorimetric sensors based on the ruthenium complexes **N719** [bis(2,2'-bipyridyl-4,4'-dicarboxylate)ruthenium(II) bis(tetrabutylammonium) bis(thiocyanate)] and **N749** [(2,2':6',2''-terpyridine-4,4',4''-tricarboxylate)ruthenium(II) tris(tetrabutylammonium) tris(isothiocyanate)] are described. It was found that mercury ions coordinate reversibly to the sulfur atom of the dyes' NCS groups. This interaction induces a color change in the dyes at submicromolar concentrations of mercury. Furthermore, the color change of these dyes is selective for mercury(II) when compared with other ions such as lead(II), cadmium(II), zinc(II), or iron(II). The detection limit for mercury(II) ions—using UV–vis spectroscopy—in homogeneous aqueous solutions is estimated to be ~20 ppb for **N719** and ~150 ppb for **N749**. Moreover, the sensor molecules can be adsorbed onto high-surface-area mesoporous metal oxide films, allowing reversible heterogeneous sensing of mercury ions in aqueous solution. The results shown herein have important implications in the development of new reversible colorimetric sensors for the fast, easy, and selective detection and monitoring of mercuric ions in aqueous solutions.

Introduction

Over the past half-century, global mercury emissions have increased substantially due mainly to natural processes¹ and emissions from coal-burning power plants and gold mining.² This volatile metal has a relatively long atmospheric residence time, which results in long-range transport and homogenization on a hemispherical scale. In aqueous solution, bacteria can transform mercury into methylmercury,³ a potent neurotoxin, which accumulates in seafood entering the food chain.^{4–6} When ingested by humans, methylmercury triggers several serious disorders including sensory, motor, and neurological damage.⁷ For example, when ingested by a pregnant woman, methylmercury readily crosses the placenta and targets the developing fetal brain and central nervous system, which can cause developmental delays in children.^{8,9}

These environmental and health problems have prompted the development of methods for the detection and quantification of mercury in aqueous solutions—including biological fluids. Examples of chromogenic^{10–16} and luminescent^{17–34} chemical

[†] Universitat de València.

[‡] Imperial College London.

[§] ICREA and ICIQ.

^{||} Swiss Federal Institute of Technology.

(1) Boening, D. W. *Chemosphere* **2000**, *40*, 1335–1351.

(2) Malm, O. *Environ. Res.* **1998**, *77*, 73–78.

(3) Harris, H. H.; Pickering, I.; George, G. N. *Science* **2003**, *301*, 1203.

(4) Nendza, M.; Herbst, T.; Kussatz, C.; Gies, A. *Chemosphere* **1997**, *35*(11), 1875–1885.

(5) Renzoni, A.; Zino, F.; Franchi, E. *Environ. Res.* **1998**, *77*, 68–72.

(6) Llobet, J. M.; Falcó, G.; Casas, C.; Teixidó, A.; Domingo, J. L. *J. Agric. Food Chem.* **2003**, *51*, 838–842.

(7) Harada, M. *Crit. Rev. Toxicol.* **1995**, *25*, 1–25.

(8) Grandjean, P.; Weihe, P.; White, R. F.; Debes, F. *Environ. Res.* **1998**, *77*, 165–172.

(9) Matsumoto, H.; Koya, G.; Takeuchi, T. *J. Neuropathol. Exp. Neurol.* **1965**, *24*, 563–574.

(10) Choi, M. J.; Kim, M. Y.; Chang, S. K. *Chem. Commun.* **2001**, 1664–1665.

(11) Moon, S. Y.; Cha, N. R.; Kim, Y. H.; Chang, S. K. *J. Org. Chem.* **2004**, *69*, 181–183.

(12) Ros-Lis, J. V.; Martínez-Mañez, R.; Rurack, K.; Sancenón, F.; Soto, J.; Spieles, M. *Inorg. Chem.* **2004**, *43*, 5183–5185.

(13) Sancenón, F.; Martínez-Mañez, R.; Soto, J. *Chem. Commun.* **2001**, 2262–2263.

(14) Sancenón, F.; Martínez-Mañez, R.; Soto, J. *Tetrahedron Lett.* **2001**, *42*, 4321–4323.

(15) Vaidya, B.; Zak, J.; Bastiaans, G. J.; Porter, M. D.; Hallman, J. L.; Nabulsi, N. A.; Utterback, M. D.; Srtzelbicka, B.; Bartsch, R. A. *Anal. Chem.* **1995**, *67*, 4101–4111.

(16) Winkler, J. D.; Bowen, C. M.; Michelet, V. *J. Am. Chem. Soc.* **1998**, *120*, 3237–3242.

(17) Aragoni, M. C.; Arca, M.; Demartin, F.; Devillanova, F. A.; Isaia, F.; Garau, A.; Lippolis, V.; Jalali, F.; Papke, U.; Shamsipur, M.; Tei, L.; Yari, A.; verani, G. *Inorg. Chem.* **2002**, *41*, 6623–6632.

(18) Baxter, P. N. W. *Chem.—Eur. J.* **2002**, *8*, 5250–5264.

(19) Cha, N. R.; Kim, M. Y.; Choe, J. I.; Chang, S. K. *J. Chem. Soc., Perkin Trans. 2* **2002**, 1193–1196.

(20) Chang, W. H.; Yang, R. H.; Wang, K. M. *Anal. Chim. Acta* **2001**, *444*, 261–269.

(21) Descalzo, A. B.; Martínez-Mañez, R.; Radeaglia, R.; Rurack, K.; Soto, J. *J. Am. Chem. Soc.* **2003**, *125*, 3418–3419.

(22) Guo, X.; Qian, X.; Jia, L. *J. Am. Chem. Soc.* **2004**, *126*, 2272–2273.

(23) Hennrich, G.; Sonnenschein, H.; Resch-Genger, U. *J. Am. Chem. Soc.* **1999**, *121*, 5073–5074.

(24) Nolan, E. M.; Lippard, S. J. *J. Am. Chem. Soc.* **2003**, *125*, 14270–14271.

(25) Ono, A.; Togashi, H. *Angew. Chem., Int. Ed.* **2004**, *43*, 4300–4302.

(26) Plaschke, M.; Czolk, R.; Ache, H. *J. Anal. Chim. Acta* **1995**, *304*, 107–113.

sensors, electrochemical devices,^{35–37} biosensors,³⁸ and sensors based on mass changes^{39,40} have been reported over the past few years. However, most of these systems still have important limitations in their limit of quantification and selectivity and typically require expensive and sophisticated equipment. For example, devices based on thin-film gold layers have been used to detect mercury^{41,42} but operate at relatively high temperatures (150–300 °C) and require, for substantial sensitivity, complicated electronic circuits; most sensors based on simple organic luminophores can usually only function in organic solvents, and often need long equilibration times for quantitative detection; biosensing of Hg²⁺ also has its limitations, requiring the use of buffering solutions and long equilibration times before the reading can be carried out.³⁸

We have recently reported that the ruthenium dye bis(2,2'-bipyridyl-4,4'-dicarboxylato)ruthenium(II) bis(tetrabutylammonium) bis(thiocyanate) (known as the **N719** dye), when supported on nanoporous TiO₂ films, changes color from dark red-purple to orange in the presence of parts per million concentrations of mercury(II) salts.⁴³ Interestingly, the color change is not observed in the presence of higher concentrations of other metals identified by the U.S. Environmental Protection Agency as potential environmental water pollutants⁴⁴ such as Zn²⁺, Cd²⁺, Ni²⁺, and Fe²⁺.

This color change coupled with the selectivity of the system for mercury(II) allowed us to demonstrate simple “naked eye” colorimetric dip sensing of mercury ions in aqueous solution. In this paper, we report our recent investigations on the chemical origin of this colorimetric mercury sensing and its dependence upon the chemical composition of the molecular sensor. We speculated in our initial studies that this sensing was associated with the presence of the thiocyanate groups on the **N719** dye, although we were not initially able to elucidate the chemical nature of any thiocyanate–mercury ion interaction. As reported herein the observed color change is indeed a consequence of the direct coordination of mercury(II) ions to the sulfur atom of the NCS groups, as shown by an X-ray crystallographic study. Further limitations of our initial study were that the mercury–dye interaction appeared irreversible and resulted in only a modest color change. These two limitations have now been

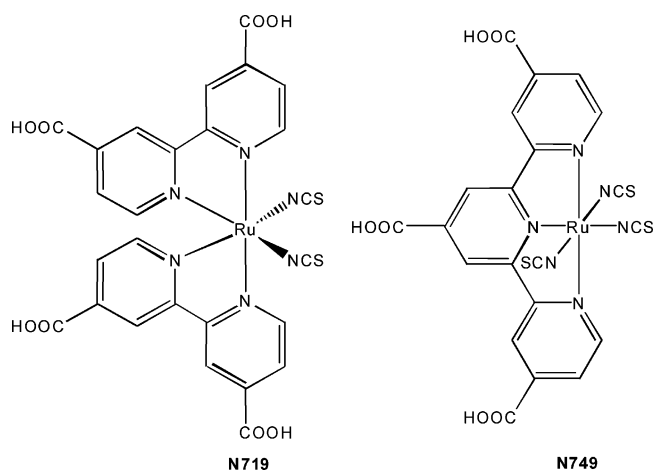


Figure 1. Chemical structure of the molecular probes **N719** and **N749**.

tackled; more specifically we have found that upon addition of iodide ions to the mercury–dye complex the mercury ion can be removed and the solid-supported molecular probe reused for sensing. On the other hand, the improvement of the color response upon mercury coordination has also been investigated by employing the molecular probe **N749**⁴⁵ (see Figure 1).

We believe that the improvement in the color response, the limit of quantification, and the reversibility in the sensing of these molecular probes will make this approach a very promising one for the analysis of mercury(II) in biological samples.

Experimental Section

Crystallographic Studies. Crystals of [Ru(N₂C₁₂O₄H₈)₂(NCS)₂·HgCl₂]·5H₂O (*M*_w = 1067.22) were obtained by slow diffusion of a water solution (15 mL) of HgCl₂ (100 mg, 0.300 mmol) layered with an acetonitrile solution (10 mL) of **N719** (20 mg, 0.017 mmol). Prismatic well-shaped orange crystals grew after several days in the dark. These crystals are sensitive to solvent loss and out of the mother liquor become brittle and finally break up after a few hours. An orange prismatic crystal (0.3 × 0.1 × 0.1 mm) of the **N719**–HgCl₂ complex was picked from its mother liquor, secured on a glass fiber tip, and mounted on a Kappa CCD Smart X-ray diffractometer equipped with graphite-monochromated Mo Kα radiation (λ = 0.71073 Å). All frames were collected at 180 K to avoid solvent loss and integrated and data corrected for absorption using the KappaCCD software package (MAXUS). The structure was solved by direct methods using the SIR97 program and refined on *F*² with the SHELXL-97 program. A total of 9359 unique reflections were collected. The crystal system was determined to be triclinic *P* $\bar{1}$, with unit cell parameters *a* = 8.8369(3) Å, *b* = 15.2570(7) Å, *c* = 17.4370(7) Å, α = 79.554(2)°, β = 86.526(1)°, γ = 80.798(2)°, and *V* = 2280.8(2) Å³; for *Z* = 2, ρ_{calcd} = 1.554 g/cm³. All non-hydrogen atoms were located after successive Fourier difference maps, and also some of the H atoms from the carboxylic groups. The rest were located in their calculated positions, and for all H atoms their thermal parameters were fixed to be 50% larger than those of the atoms to which they are bound. According to the data, the positions corresponding to the Hg centers were refined at half-occupancy. The carboxylic groups also showed positional disorder over two possible positions, and this was best modeled by assigning half-occupancy to each position. The solvent areas were modeled to disordered oxygen atoms from water molecules. All non-hydrogen atoms were refined anisotropically, except the disordered carboxylic

- (27) Prodi, L.; Bargossi, C.; Montalti, M.; Zaccheroni, N.; Su, N.; Bradshaw, J. S.; Izatt, R. M.; Savage, P. B. *J. Am. Chem. Soc.* **2000**, *122*, 6769–6770.
 (28) Rurack, K.; Kollmannsberger, M.; Resch-Genger, U.; Daub, J. *J. Am. Chem. Soc.* **2000**, *122*, 968–969.
 (29) Sakamoto, H.; Ishikawa, J.; Nakao, S.; Wada, H. *Chem. Commun.* **2000**, 2395–2396.
 (30) Sandor, M.; Geistmann, F.; Schuster, M. *Anal. Chim. Acta* **1999**, *388*, 19–26.
 (31) Sasaki, D. Y.; Padilla, B. E. *Chem. Commun.* **1998**, 1581–1582.
 (32) Yoon, J.; Ohler, N. E.; Vance, D. H.; Aumiller, W. D.; Czarnick, A. W. *Tetrahedron Lett.* **1997**, *38*, 3845–3848.
 (33) Zhang, X. B.; Guio, C. C.; Li, Z. Z.; Shen, G. L.; Yu, R. Q. *Anal. Chem.* **2002**, *74*, 821–825.
 (34) Chae, M. Y.; Czarnick, A. W. *J. Am. Chem. Soc.* **1992**, *114*, 9704–9705.
 (35) Marzouk, S. A. M.; Al-Arjiqui, W. T.; Hassan, S. S. *Anal. Bioanal. Chem.* **2003**, *375*, 1186–1192.
 (36) Mashhadizadeh, M. H.; Sheikshoiae, I. *Talanta* **2003**, *60*, 73–80.
 (37) Yantasee, W.; Lin, Y.; Zemanian, T. S.; Fryxell, G. E. *Analyst* **2003**, *128*, 467–472.
 (38) Shi, G. Q.; Jiang, G. *Anal. Sci.* **2002**, *18*, 1215–1219.
 (39) Manganiello, L.; Rios, A.; Valcarcel, M. *Anal. Chem.* **2002**, *74*, 921–925.
 (40) Xu, X.; Thundat, T. G.; Brown, G. M.; Ji, H. F. *Anal. Chem.* **2002**, *74*, 3611–3615.
 (41) Brainina, K. Z.; Stozhko, N. Y.; Shalygina, Z. V. *J. Anal. Chem.* **2002**, *57*, 945–949.
 (42) McNerney, J. J.; Buseck, P. R.; Hanson, R. C. *Science* **1972**, *178*, 611–612.
 (43) Palomares, E.; Vilar, R.; Durrant, J. R. *Chem. Commun.* **2004**, 362–363.
 (44) For an update on water contaminants see www.epa.gov/safewater/hfacts.html.

- (45) Nazeeruddin, M. K.; Péchy, P.; Renouard, T.; Zakeeruddin, S. M.; Humphry-Baker, R.; Comte, P.; Liska, P.; Le, C.; Costa, E.; Shklover, V.; Spiccia, L.; Deacon, G. B.; Bignozzi, C. A.; Gratzel, M. *J. Am. Chem. Soc.* **2001**, *123*, 1613–1624.

groups and solvent molecules. Final refinement for 6330 reflections [$I > 2\sigma(I)$] and 521 parameters gave $R1 = 0.0624$ and $wR2 = 0.1428$ ($GOF = 1.004$).⁴⁶ However, we note that, depending on the relative concentration of species in solution, other compounds can be formed. In particular, we found that the first solid precipitate that appears at the limit of low Hg concentration/precipitate formation showed a Ru:Hg ratio of 3:2, different from the 1:1 ratio found in the crystalline solid isolated. This microanalysis was performed with a JEOL 6300 microscope equipped with an EDAX analysis system.

Spectroscopic Studies in Solution. The **N719** and **N749** molecular probes were dissolved in ethanol (HPLC grade) to obtain a 20 μM stock solution. The mercury(II) quantification experiments were carried out on a quartz cuvette with a total volume of 3 mL. The mercury(II) aliquots were injected into the quartz cuvette from a 1 mM HgCl_2 aqueous stock solution. The changes in the UV-vis absorption spectra were monitored at room temperature using a double-beam UV-vis spectrophotometer, Shimadzu Uv-1601.

Preparation of Sensitized Nanoporous TiO_2 Films. The mesoporous, nanocrystalline TiO_2 films comprising 15 nm sized anatase TiO_2 particles were prepared as follows: 20 mL of titanium isopropoxide was injected into 4.5 g of glacial acetic acid under an argon atmosphere and the mixture stirred for 10 min. The mixture was then injected into 120 mL of 0.1 M nitric acid under an argon atmosphere at room temperature in a conical flask and the resulting mixture stirred vigorously. After the nitric acid addition, the flask was left uncovered and heated at 80 $^\circ\text{C}$ for 8 h. After cooling, the solution was filtered using a 0.45 μm syringe filter, diluted to 5wt % TiO_2 by the addition of H_2O , and then autoclaved at 220 $^\circ\text{C}$ for 12 h. The colloids were redispersed with a 60 s cycle burst from an LDU Soniprobe horn as reported before. The solution was then concentrated to 12.5% on a rotary evaporator using a membrane vacuum pump at 40 $^\circ\text{C}$. Carbowax 20000 (6.2 wt %) was added, and the resulting paste was stirred slowly overnight to ensure homogeneity. The suspension was spread on the substrates by a glass rod, using 3M adhesive tapes as spacers. After the films were dried in air, they were sintered at 450 $^\circ\text{C}$ for 20 min in air. The thickness of the TiO_2 films was controlled, resulting in a film thickness of 4 μm .

Spectroscopic Measurement of **N749 Supported on Mesoporous Nanocrystalline TiO_2 Films.** The **N749** dye was adsorbed onto a 4 μm thick nanoporous, optically transparent TiO_2 film by soaking the film in a 1 mM solution of the dye in a 1:1 mixture of acetonitrile/*tert*-butyl alcohol at room temperature overnight, followed by rinsing in ethanol to remove unadsorbed dye, resulting in a strong green-black coloration of the film (as illustrated in Figure 4). The dye loading, determined from the optical density of **N749** observed for the mesoporous nanocrystalline TiO_2 film at the **N749** absorption maximum (600 nm), was estimated as $\sim 95\%$ monolayer coverage.

Mercury(II) quantification experiments were carried out on a quartz cuvette with a total volume of 3 mL. The **N749**-sensitized TiO_2 film was immersed in the aqueous solution and the cuvette fixed to the UV-vis spectrophotometer holder. The UV-vis absorption spectra were recorded after addition of the corresponding cation with an equilibration time before the measurement of 2 min. Experiments were conducted in unbuffered aqueous solutions, unless otherwise stated. Studies as a function of solution pH employed an aqueous solution starting at pH 3.0 and increasing the amount of base until pH 8.0 was reached. pH measurements in nonaqueous media (acetonitrile) were carried out using an HI 8424 microcomputer pH meter glass electrode. The calibration was performed according to the literature method.

The reversibility experiments were performed by dipping the **N719**-sensitized TiO_2 film ($\sim 1 \text{ cm}^2$ area) into a solution containing a $1 \times 10^{-3} \text{ M}$ cation concentration. After dipping, the UV-vis absorption

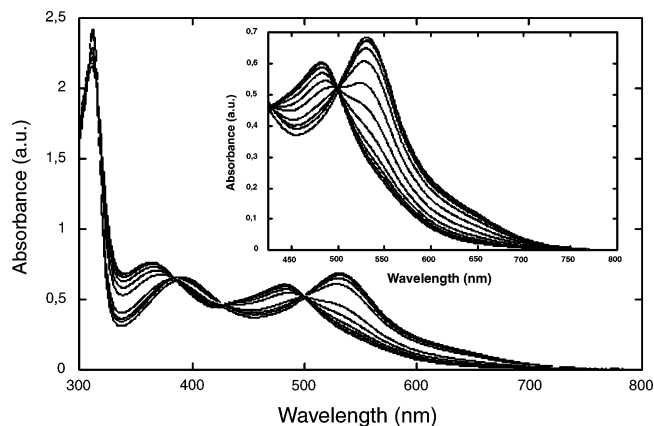


Figure 2. Changes in the UV-vis absorption spectra of a 2 mL solution from a 20 μM stock solution of **N719** upon addition of increasing amounts of mercury(II). The inset shows the absorption maximum shift in the visible region.

spectrum was measured, and finally, the sample was dipped into a vial containing 10 mM KI in distilled water and dried at 40 $^\circ\text{C}$. The same sample was used in repeating cycles without appreciable dye desorption. However, it is noteworthy that the samples show less efficient reversibility after six cycles.

Results and Discussion

Investigations of the Mercury–N719** Dye Interaction: Solution and X-ray Studies.** To investigate the origin of the observed color change of the TiO_2 -supported **N719** dye in the presence of mercury(II) ions, we decided to investigate the process in solution (with the hope of isolating a dye–mercury(II) complex). As expected, when different amounts of Hg^{2+} were added to an aqueous solution of **N719**, the color change of the solution (from dark red-purple to orange) could be seen by naked eye inspection (down to 1.5 ppm). To have a more quantitative measure of this change, the aqueous solution of **N719** was titrated with a solution of HgCl_2 and the UV-vis absorption spectra were recorded. As shown in Figure 2, upon addition of the metal salt to the dye, the absorption at 530 nm decreases while that at 480 nm increases. The limit of quantification in solution ($\sim 20 \text{ ppb}$) is even lower than that observed when the dye is supported on the TiO_2 nanoporous film.

Once it was confirmed that the ruthenium dye also changes its color in solution and not only when deposited onto the TiO_2 film, we engaged in understanding the molecular interaction responsible for the change in the optical properties of the dye. Besides the color change, it was observed by IR spectroscopy that, upon addition of HgCl_2 to an aqueous solution of **N719**, the peak for the C=N stretching frequency corresponding to the NCS group was reduced in intensity and shifted from 2112 to 2150 cm^{-1} , suggesting the existence of an interaction between the mercury(II) ions and this group. To gain a better understanding of this interaction, single crystals suitable for an X-ray crystallographic study were obtained by layering an aqueous solution of HgCl_2 with a solution of **N719** in acetonitrile. The structural characterization showed that the mercury(II) ions coordinate to the sulfur of the NCS groups from different **N719** molecules (see Figure 3a). Thiocyanates are ligands well-known to form $\text{M}-\text{S}=\text{C}=\text{N}-\text{M}'$ bridges. A large number of complexes have been previously reported in which one of the metal centers being bridged is mercury.^{47–52} In contrast, more limited literature is available when one of the metal centers is ruthenium.^{53–56}

(46) CCDC-259514 contains the supplementary crystallographic data for this paper. These data can be obtained free of charge via www.ccdc.cam.ac.uk/conts/retrieving.html (or from the Cambridge Crystallographic Data Centre, 12 Union Rd., Cambridge CB2 1EZ, U.K.; fax +44-1223-336-033; e-mail deposit@ccdc.cam.ac.uk).

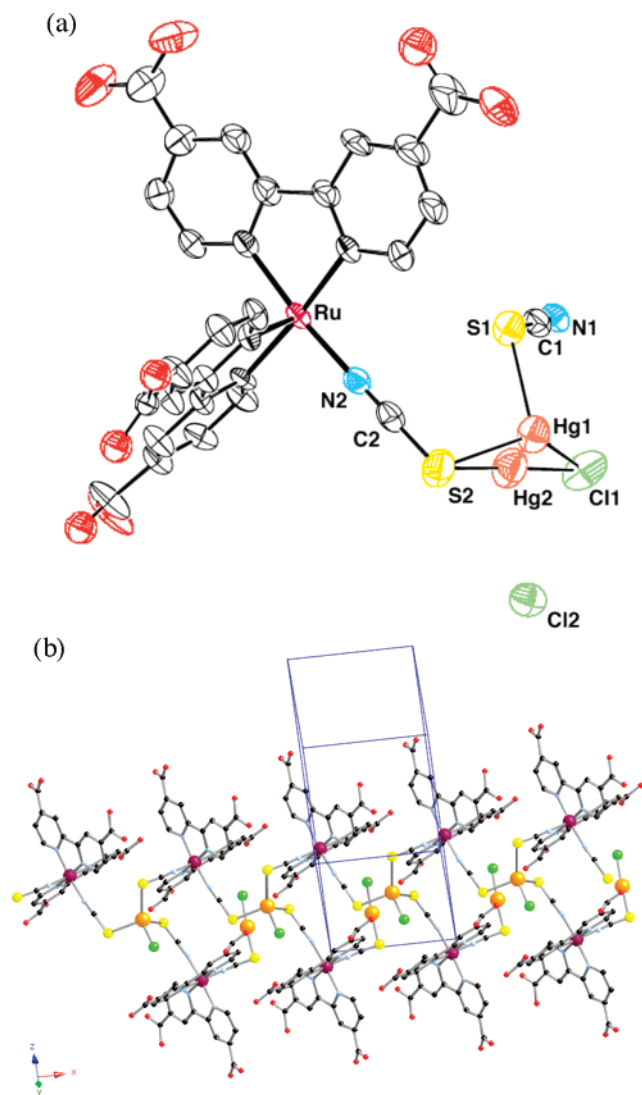


Figure 3. Molecular structure of the N719–HgCl₂ complex showing (a) the asymmetric unit which contains one mercury atom, crystallographically disordered in two positions at half-occupancy, one [Ru(N₂C₁₂O₄H₈)₂(NCS)₂] complex, and two Cl[−] anions (disordered atoms from the carboxylic units and H atoms have been omitted for clarity) and (b) a representation of the structure of the [Ru(N₂C₁₂O₄H₈)₂(NCS)₂HgCl]_n⁺ chains parallel to the *a* axis.

The asymmetric unit contains one mercury atom, crystallographically disordered in two positions at half-occupancy, one Ru(N₂C₁₂O₄H₈)₂(NCS)₂ complex, and two Cl[−] anions. One of the mercury positions (Hg1) is tetrahedrally coordinated to three

sulfur atoms from three different adjacent ruthenium complexes and one Cl[−] anion, with mercury-to-ligand distances between 2.463(2) Å for the Hg1–Cl1 bond and 2.578(2) Å for the longest Hg1–S1 coordination bond. The angles are close to regular tetrahedral, except for two of the Cl–Hg–S angles, which deviate to 131.2(1)° (Cl1–Hg1–S2) and 96.41(7)° (Cl1–Hg1–S1). On the other hand, Hg2 presents a linear coordination, bound to one sulfur and one Cl[−] anion, with much shorter bond distances (Hg2–S2 = 2.289(2) Å and Hg2–Cl1 = 2.268(2) Å). The two mercury positions are just about 1 Å apart, which clearly indicates that both positions cannot be occupied at the same time, while the Cl1 atom, with an occupancy of one, coordinates both positions, whichever mercury atom is present locally. All thiocyanate ligands from the ruthenium complexes coordinate also to a mercury atom, with S1 coordinating only Hg1 positions, and with S2 coordinating to either Hg1 or Hg2, depending on the given local distribution. The growth of the asymmetric unit gives rise to chains that run parallel to the *a* axis (Figure 3b).⁵⁷

Between chains there are several short contacts between carboxylate groups that correspond to strong hydrogen bonding. The O–O distances, as short as 2.5 Å, are clear evidence that the carboxylate groups are protonated. All protons from these groups were located (see the Experimental Section and Supporting Information), even when the carboxylate groups show some disorder over two adjacent positions that deviate slightly, below or above, from the planar bipyridine rings.

These cationic chains of formula [Ru(N₂C₁₂O₄H₈)₂(NCS)₂HgCl]_n⁺ leave large empty channels running also along the *a* axis that constitute over 35% of the unit cell volume. These channels are occupied by free Cl[−] anions required for electro-neutrality and disordered solvent molecules, assigned to water. This explains the instability of the crystals, since the crystallization solvent molecules rapidly leave the structure at ambient pressure, provoking a structural collapse.

The formulation shown by X-ray crystallography of the N719–mercury(II) complex is consistent with the elemental analyses of the bulk sample. However, it should be noted that this crystalline solid is an insoluble coordination polymer and hence is not likely to be the complex directly responsible for the changes observed in solution. The crystallographic evidence however strongly suggests that at low concentrations of mercury(II) and N719 dye, a molecular complex (involving NCS–mercury interactions) must be formed. Only at higher concentration and after long periods of time is the coordination polymer formed. From the structural point of view, this is the

- (47) Ahuja, I. S.; Garg, A. J. *Inorg. Nucl. Chem.* **1972**, *34*, 1929–1935.
 (48) Davis, A. R.; Murphy, C. J.; Plane, R. A. *Inorg. Chem.* **1970**, *9*, 423–425.
 (49) Madalan, A. M.; Kravtsov, V. C.; Pajic, D.; Zadro, K.; Simonov, Y. A.; Stanica, N.; Ouahab, L.; Lipkowski, J.; Andruh, M. *Inorg. Chim. Acta* **2004**, *357*, 4151–4164.
 (50) Ricciari, P.; Zinato, E.; Rievaj, M.; Bustin, D.; Mesaros, S. *Inorg. Chim. Acta* **1997**, *255*, 229–237.
 (51) Wang, X. Q.; Xu, D.; Lu, M. K.; Yuan, D. R.; Xu, S. X.; Guo, S. Y.; Zhang, G. H.; Liu, J. R. *J. Cryst. Growth* **2001**, *224*, 284–293.
 (52) Wang, X. Q.; Xu, D.; Lu, M. K.; Yuan, D. R.; Cheng, X. F.; Huang, J.; Wang, S. L.; Yu, W. T.; Sun, H. Q.; Duan, X. L.; Ren, Q.; Yang, H. L. *Chem. Phys. Lett.* **2003**, *367*, 230–237.
 (53) Bruce, M. I.; Cooke, M.; Green, M. *J. Organomet. Chem.* **1968**, *13*, 227–234.
 (54) Hsu, S.-C.; Lin, Y.-C.-L.; Huang, S.-L.; Liu, Y.-H.; Wang, Y.; Liu, H. *Eur. J. Inorg. Chem.* **2004**, 459–462.
 (55) Natarajan, K.; Poddar, R. K.; Agarwala, U. *J. Inorg. Nucl. Chem.* **1977**, *39*, 431–435.
 (56) Poddar, R. K.; Parashad, R.; Agarwala, U. *J. Inorg. Nucl. Chem.* **1980**, *42*, 837–838.

- (57) In principle, two possible structural features can be the origin for the crystallographic disorder found for the Hg centers. The structure can be formed by one-dimensional chains following a –S1–Hg1–S1–Hg1– core, as we propose, with each Hg completing its tetrahedral coordination with S2 and Cl1. This leaves one noncoordinated S2 atom, which binds the second Hg2 atom, in linear coordination with Cl1. From such a chain, where all the tetrahedral Hg centers are aligned, the crystallographic disorder would come from the random distribution of the chains in the overall packing, since no given order should exist about how the metal centers are distributed. The other possibility would include a random distribution of the Hg centers in a given chain, which would also result in the same crystallographic disorder, but in such a case, a chain would not exist, since with a random zigzag distribution of the Hg1 centers only short oligomers would occur, with the shortest one including four Hg atoms. Although this is possible, it is difficult to justify such a random distribution along the chain, which would imply the presence of oligomers of different lengths in the same crystal. Although crystallographically equivalent, such a chemical composition would probably not give rise to this crystal packing. Indeed, no interactions are observed in the crystal structure that would favor its formation. Thus, only the presence of the infinite –S1–Hg1–S1–Hg1– chain allows us to understand the crystal structure found.

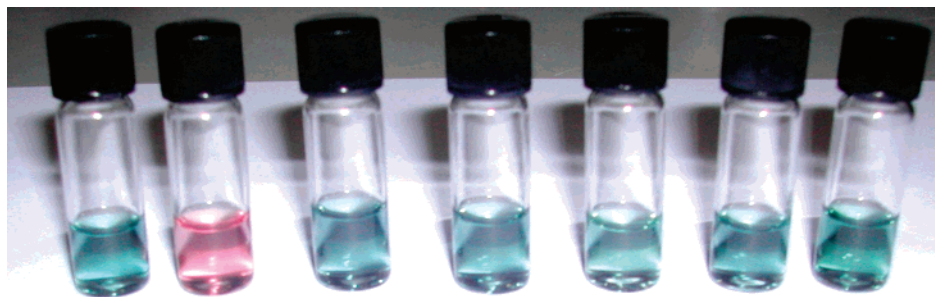


Figure 4. From left to right, no metal, Hg^{2+} , Cd^{2+} , Pb^{2+} , Fe^{2+} , Cu^{2+} , and Zn^{2+} . All metals were added in the same equimolar amounts (~ 13 ppm) from aqueous solutions of their respective salts to 1 mL of **N749** dissolved in ethanol.

first example of a compound where linear and tetrahedral mercury(II) centers coexist and the first time a linear coordination mode is observed with a thiocyanate ligand. The crystal structure of HgCl_2 is essentially linear. Linear coordination is also favored in organometallic compounds, such as in methylmercury derivatives⁵⁸ or phosphine complexes.⁵⁹ When coordinated by sulfur atoms, the geometry of molecular mercury(II) complexes depends on the nature of the ligands and also of the solvents used for crystal growth. A large variety of geometries have been reported, including linear, trigonal planar, tetrahedral, trigonal bipyramidal, and octahedral.⁶⁰ Thiols usually favor tetrahedral or linear coordination, with bulky thiols usually imposing the latter.⁶¹

In regard to thiocyanate complexes, mercury is known to bind preferentially to the sulfur side, as in the discrete tetrahedral $[\text{Hg}(\text{SCN})_4]^{2-}$ anion,⁶² which also appears in solid-state materials with interesting optical properties,⁶³ where the N side of the thiocyanate binds first-row-transition-metal centers. In all cases, the thiocyanate binding mode to mercury is not linear, with the C–S–Hg angle far from 180° . The reported compounds where mercury(II) is coordinated by thiocyanate and halide ligands adopt tetrahedral or pseudooctahedral geometries for the mercury centers.⁶⁴ Moreover, this is also the first example where a μ -1,1-thiocyanate bridge between mercury(II) atoms has been observed. Several examples with μ -1,3-thiocyanate bridges are known where thiocyanate binds mercury(II) atoms by the sulfur and nitrogen ends, as in the dimer $[\text{Hg}(\text{SCN})(\text{NO}_3)(\text{PBz}_3)]_2$ (PBz = tribenzylphosphine)⁵⁹ or in the polymer⁶⁵ $[\text{Hg}(\text{SCN})_3]^-$. A μ -1,1 bridging mode has been found for the analogous azide ligand.⁶²

Studies of the Interaction between Mercury(II) and the Ruthenium Dye N749. Having established that the coordination of mercury(II) to the dye's NCS groups is responsible for the observed color change, we decided to investigate further other NCS-containing dyes. The idea was to find a dye that would respond in an analogous manner to the presence of mercury(II)

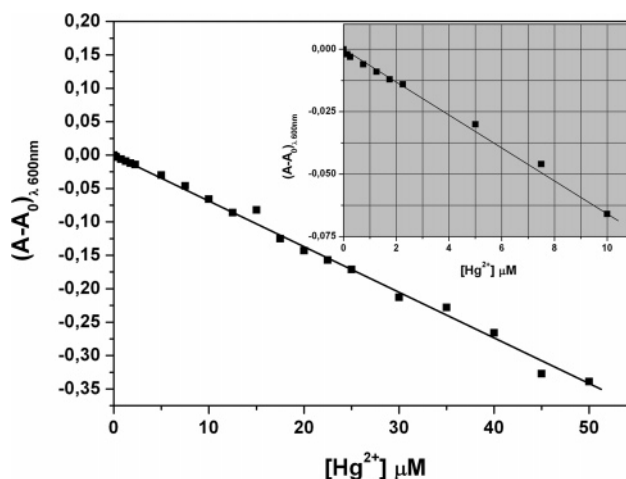


Figure 5. Titration of the change in the absorption of **N749** in ethanol measured at $\lambda = 600$ nm versus the concentration of added Hg^{2+} ions. The inset shows the amplification of the graph for the low-limit colorimetric response for mercury. The mercury was added from a stock HgCl_2 aqueous solution.

but showing a bigger color change to make the naked eye detection easier. In particular, the interaction between mercury(II) salts and the complex (2,2':6',2''-terpyridine-4,4',4''-tricarboxylate)ruthenium(II), tris(tetrabutylammonium) tris(isothiocyanate) (**N749**) was investigated. This was first investigated in solution by adding different cations (namely, Hg^{2+} , Cd^{2+} , Pb^{2+} , Fe^{2+} , Cu^{2+} , and Zn^{2+}) to a solution of the **N749** dye. As is shown in Figure 4, the ruthenium complex undergoes a dramatic color change from dark green to pink upon addition of HgCl_2 salts but not in the presence of any other of the tested metal cations.

Once the selectivity of the **N749** dye for Hg^{2+} was established, it was of interest to determine the limit of quantification for the detection of mercury(II). The solutions of the green-black ruthenium complex were titrated with HgCl_2 , showing that upon addition of increasing amounts of the mercury(II) salt the charge-transfer band centered at $\lambda = 625$ nm decreased while a new band appeared at $\lambda = 560$ nm. As can be seen in Figure 5, the dye has a linear response to increasing amounts of mercury(II) (between 0.5 and 60 nmol). From this plot it is also possible to establish that the system has a limit of quantification down to ~ 100 ppb.

We next proceeded to support the **N749** dye on a nanoporous TiO_2 film and measured the ability of the sensitized film to detect mercury(II) salts in aqueous solution. The ruthenium complex **N749** was adsorbed onto a 4 μm thick mesoporous TiO_2 film by soaking the film in a 1 mM solution of the dye in

- (58) Brownlee, R. T. C.; Cauty, A. J.; Mackay, M. F. *Aust. J. Chem.* **1978**, *31*, 1933–1936.
 (59) Bowmaker, G. A.; Assadollahzadeh, B.; Brodie, A. M.; Ainscough, E. W.; Freeman, G. H.; Jameson, G. B. *Dalton Trans.* **2005**, 1602–1612.
 (60) Dance, I. G. *Polyhedron* **1986**, *5*, 1037–1104.
 (61) Block, E.; Brito, M.; Gernon, M.; McGowty, D.; Kang, H.; Zubieta, J. *Inorg. Chem.* **1990**, *29*, 3172–3181.
 (62) Chand, B. G.; Ray, U. S.; Mostafa, G.; Cheng, J.; Lu, T.-H.; Shinha, C. *Inorg. Chim. Acta* **2005**, *358*, 1927–1933.
 (63) Wang, X. Q.; Xu, D.; Lu, M. K.; R., Y. D.; Xu, S. X. *Mater. Res. Bull.* **2001**, *36*, 879–887.
 (64) Mosset, A.; Bagieu-Beucher, M.; Lecchi, A.; Masse, R.; Zaccaro, J. J. *Solid State Sci.* **2001**, *4*, 827–824.
 (65) Pichardt, J.; Gong, G.-T.; Hoffmeister, I. *Z. Naturforsch., Teil B* **1995**, *50*, 993–996.

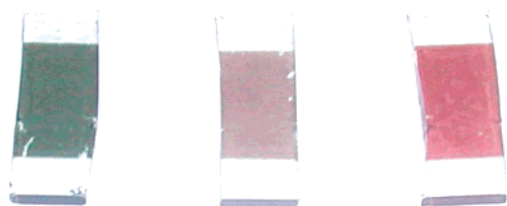


Figure 6. Mesoporous nanocrystalline TiO₂ sensitized with N749 before (left) and after immersion in 9 ppm HgCl₂ in distilled water for 1 h (center) and 300 ppm HgCl₂ in distilled water for 5 min (right).

a 1:1 mixture of acetonitrile/*tert*-butyl alcohol at room temperature overnight. The cation-sensing experiments with the TiO₂–N749 films were carried out in distilled water (pH ≈ 5) by exposing the films to micromolar solutions of the metal cations under study (i.e., Hg²⁺, Cd²⁺, Pb²⁺, Fe²⁺, Cu²⁺, and Zn²⁺). As observed in the solution studies, the supported N749 dye only changed color when dipped into the mercury(II) solution (see Figure 6). Using the N749-sensitized TiO₂ film, it is hence possible to detect low parts per million levels of mercury(II) in water by naked eye inspection.

Studies on the Reversibility of Mercury(II) Binding to TiO₂–N719 Films. For a chemical sensor to be widely employed in the detection of specific analytes, the limit of quantification, selectivity, and reversibility are all important aspects. Both molecular probes herein presented have demonstrated to be sensitive (in the parts per billion region) and selective (even in the presence of competing metals) for the detection of mercury(II) salts. Consequently, it was of great interest to investigate the reversibility of the system. For this, a mesoporous nanocrystalline TiO₂ film sensitized with N719 was first exposed to a 1 mM solution of HgCl₂ in water; the resulting orange film (due to the interaction of the mercury(II) cations with the NCS groups of the ruthenium complex) was subsequently dipped into a 10 mM solution of KI. This generated an immediate color change of the film back to the red color characteristic of the TiO₂–N719 film before it was exposed to mercury(II). If this film is subsequently dipped again into the HgCl₂ solution, the color of the film changes to orange once

again. This procedure can be repeated several times, demonstrating that the supported dye can be reutilized by dipping it into an iodide solution.

The mechanism by which this process occurs is likely to involve the formation of a stable mercury–iodide complex that displaces the mercury from the ruthenium complex.

Conclusion

The results presented in this paper demonstrate that the interaction between mercury(II) ions and the NCS groups of the ruthenium dyes N719 and N749 is responsible for the color change of the corresponding dye. Interestingly, the interaction is selective for mercury(II) even in the presence of much higher concentrations of other potentially competing metal cations—such as lead(II), cadmium(II), zinc(II), or iron(II). Furthermore, the limit of quantification of the system—using UV–vis spectroscopy—in homogeneous aqueous solutions is estimated to be ~20 ppb for N719 and ~150 ppb for N749, providing a good chemosensor for this toxic metal. By supporting these dyes on mesoporous TiO₂ films, we have developed an easy-to-use system for the dip sensing of mercury(II) in aqueous solution. These films can be reutilized for sensing if they are washed with an aqueous solution of KI—which presumably removes the mercury from the surface by forming a stable iodide complex of it.

Acknowledgment. J.R.D. and E.P. thank the Imperial College London Fleming Fund for financial support. E.P. also thanks EU for Marie Curie Fellowship HPMF-CT-2002-01744. IcMol thanks the MEC (MAT 2004-3849 and C.M.-G. FPU Fellowship) and the Generalitat Valencia for financial support. M.G. and Md.K.N. acknowledge financial support of this work by the Swiss Federal Office for Energy (OFEN).

Supporting Information Available: Crystallographic data (CIF) and a movie showing the reversible colorimetric sensing of mercury ions. This material is available free of charge via the Internet at <http://pubs.acs.org>.

JA0517724